Original article

MOLECULAR METABOLISM

Lipolysis sensation by white fat afferent nerves triggers brown fat thermogenesis

John T. Garretson [1,3,*], Laura A. Szymanski [2], Gary J. Schwartz [4], Bingzhong Xue [1,2,3], Vitaly Ryu [2,3], Timothy J. Bartness [1,2,3]

ABSTRACT

Objective: Metabolic challenges, such as a cold environment, stimulate sympathetic neural efferent activity to white adipose tissue (WAT) to drive lipolysis, thereby increasing the availability of free fatty acids as one source of fuel for brown adipose tissue (BAT) thermogenesis. WAT is also innervated by sensory nerve fibers that network to metabolic brain areas; moreover, activation of these afferents is reported to increase sympathetic nervous system outflow. However, the endogenous stimuli sufficient to drive WAT afferents during metabolic challenges as well as their functional relation to BAT thermogenesis remain unknown.

Method: We tested if local WAT lipolysis directly activates WAT afferent nerves, and then assessed whether this WAT sensory signal affected BAT thermogenesis in Siberian hamsters (*Phodopus sungorus*).

Results: 2-deoxyglucose, a sympathetic nervous system stimulant, caused β-adrenergic receptor dependent increases in inguinal WAT (IWAT) afferent neurophysiological activity. In addition, direct IWAT injections of the β_3-AR agonist CL316,243 dose-dependently increased: 1) phosphorylation of IWAT hormone sensitive lipase, an indicator of SNS-stimulated lipolysis, 2) expression of the neuronal activation marker c-Fos in dorsal root ganglion neurons receiving sensory input from IWAT, and 3) IWAT afferent neurophysiological activity, an increase blocked by antilipolytic agent 3,5-dimethylpyrazole. Finally, we demonstrated that IWAT afferent activation by lipolysis triggers interscapular BAT thermogenesis through a neural link between these two tissues.

Conclusions: These data suggest IWAT lipolysis activates local IWAT afferents triggering a neural circuit from WAT to BAT that acutely induces BAT thermogenesis.

© 2016 The Author(s). Published by Elsevier GmbH. This is an open access article under the CC BY-NC-ND license (http://creativecommons.org/licenses/by-nc-nd/4.0/).

Keywords Lipolysis; Adipose innervation; WAT sensory; BAT thermogenesis; Denervation

1. INTRODUCTION

Adipose tissue is connected to the CNS via afferent and efferent nerve fibers directly innervating each fat depot. While adipose efferents are entirely catecholaminergic [1], adipose afferents are primarily unmyelinated c-fibers—positive for substance p and calcitonin gene-related peptide (CGRP)—and receptive to a variety of stimuli [2]. Although the anatomical reality of WAT afferents was initially discovered by Fishman and Dark [3], the first functional role of neural afferents arising from white adipose tissue (WAT) was demonstrated by Niijima [4] by injecting the adiposity hormone leptin directly into WAT then measuring neurophysiological activity in decentralized (sensory) nerve fibers connected to the tissue. These results have been interpreted to suggest that local leptin, secreted by WAT in proportion to adipocyte size and number, is transduced as a neural signal proportional to the amount of stored energy [5]. However, WAT afferents also increase their neurophysiological activity in response to adenosine and bradykinin—indicating an active role of these afferents in blood pressure sensation [6]. Despite the variety of signals sensed by WAT afferents, each neurophysiolgically effective stimulus similarly increases sympathetic nervous system (SNS) drive to WAT and other tissues in a positive feedback WAT-brain-SNS reflex circuit termed the "adipose afferent reflex" (AAR) [6,7]. Indeed, our viral tracing studies expose the neuroanatomical framework for this AAR wherein WAT afferents are networked to WAT efferents throughout metabolically relevant CNS nuclei (*e.g.* intermediolateral nucleus of the spinal cord, nucleus of the solitary tract, periaqueductal gray, dorsomedial, lateral, arcuate and paraventricular hypothalamus) [8]. In addition, these studies reveal a high degree of neuroanatomical overlap between neuronal populations at multiple peripheral and central levels of the neuraxis including WAT sensory and brown adipose tissue (BAT) SNS innervation [9,10]. Thus, functional and neuroanatomical sensory-motor links between WAT and the SNS have been established [11,12]; however, the sensitivity of WAT afferents to local lipolytic activity of the tissue and the potential for these afferents to induce heat production in BAT have not been investigated.

Among all functions of WAT, its catabolism and subsequent efflux of stored energy is a rapid and necessary process for the release of fuels

[1]Neuroscience Institute, Georgia State University, Atlanta, GA 30303, USA [2]Department of Biology, Georgia State University, Atlanta, GA 30303, USA [3]Center for Obesity Reversal, Georgia State University, Atlanta, GA 30303, USA [4]Department of Medicine and Neuroscience, Albert Einstein College of Medicine, Bronx, NY 10461, USA

*Corresponding author. 50 Decatur Street SE, Biology Department, Atlanta, GA 30303, USA. Tel.: +1 770 883 5804 (Daytime). E-mail: johnny.garretson@gmail.com (J.T. Garretson).

Received June 7, 2016 • Revision received June 24, 2016 • Accepted June 26, 2016 • Available online 30 June 2016

http://dx.doi.org/10.1016/j.molmet.2016.06.013

 © 2016 The Author(s). Published by Elsevier GmbH. This is an open access article under the CC BY-NC-ND license (http://creativecommons.org/licenses/by-nc-nd/4.0/).

when energy demand is high, and this process is evolutionarily conserved across species including non-mammals [13,14]. During an energetic challenge such as cold exposure, norepinephrine released by axon terminals of post ganglionic SNS neurons binds β_3-adrenorecptors (β_3-AR) present on adipocytes [15] initiating a lipolytic cascade that depends on phosphorylation of hormone sensitive lipase (HSL) and leads to the preferential release of long-chain free-fatty acids (FFAs) and glycerol as useable energy [16,17]. Peripheral injection of 2-deoxyglucose (2DG), a glucoprivic sympathomimetic agent, causes an SNS-dependent mobilization of triglycerides from WAT and increases WAT afferent activity within minutes [9]. This efflux of substrates from WAT occurs locally first, then is circulated throughout the body/brain and oxidized as fuel when glucose is not readily available/sufficient for energy demand [18] or converted to heat via uncoupled oxidative phosphorylation by BAT, a tissue similarly dependent on SNS innervation to trigger thermogenesis [42]. Thus, we hypothesize that WAT afferents activated by glucoprivation may be sensing locally released lipolytic products, thereby transducing lipolysis into rapid neural signals communicated to the CNS [9]. Such sensation of lipolysis by WAT afferents may induce BAT thermogenesis because 1) lipolysis provides substrates that are required for BAT thermogenesis [19,20] and 2) there is significant overlap in the central neuroanatomical representation of WAT afferent projections and neurons that project to BAT efferents [9,10]. To investigate these hypotheses, we first tested if WAT lipolysis and/or its products were sufficient to drive spinal afferent nerves receiving sensory input from subcutaneous inguinal WAT (IWAT), then we tested whether stimulation of lipolysis sensing IWAT afferents triggers interscapular BAT (IBAT) thermogenesis.

2. METHOD

2.1. Animals

Adult male Siberian hamsters (*Phodopus sungorus*; ~3–4 months old) from our breeding colony were individually housed in a long day photoperiod (16 h:8 h light:dark cycle; at 22 ± 2 °C) with free access to water and rodent chow. Siberian hamsters were used because of the expanding literature characterizing the anatomy of their neuro-adipose axis [13] and the apparent conservation of adipocyte catabolism among mammalian species [14]. All procedures were approved by the Georgia State University Institutional Animal Care and Use Committee and are in accordance with Public Health Service and United States Department of Agriculture guidelines.

2.2. Neurophysiological recordings of IWAT afferent nerve activity

Siberian hamsters ($n = 13$, unilateral recordings; $n = 16$, bilateral recordings) were anesthetized with ketamine (100 mg/kg)/xylazine (10 mg/kg, i.p.). Following a 2 cm dorsal ventral incision, IWAT and connective tissue was resected and isolated from surrounding tissue, after which the nerves innervating right and/or left IWAT were exposed. Single nerve bundles from these WAT nerves were isolated and severed proximal to the electrode placement site to disconnect efferent fibers, and the afferent (distal) ends of decentralized nerves were placed on platinum-iridium (32-gauge) hook electrodes. A petroleum jelly/mineral oil mixture (1:1) was applied to the sites to completely surround the electrode/nerve connection, and warm mineral oil was pooled into the recording area to insulate electrical noise, prevent aqueous infusions from leaking to other tissue, secure the nerve on the electrode, and reduce drying of tissue. A stable anesthetic plane was maintained with supplemental ketamine (50 mg/kg, s.c.) by examining toe pinch and eye blink responses throughout the recordings.

For unilateral recordings, baseline neurophysiological spike activity in IWAT afferents was recorded for 5 min as reported [9], then hamsters received either propranolol (40 mg/kg, i.p.) or sterile saline vehicle (i.p.) and spikes were recorded for an additional 5 min. Finally, 2DG (500 mg/kg, s.c.) was administered and IWAT afferent activity was measured for an additional 10 min.

For bilateral neurophysiological recordings, decentralized nerve bundles from left and right IWAT were each placed on electrodes, then three sharp stainless steel needles connected with Silastic tubing to Hamilton microsyringes (Hamilton Company, Reno, NV) were inserted into left and right IWAT along the lateral-coronal plane spaced 4–5 mm apart at a depth of approximately 4–5 mm each (diagram of procedure, Figure 2A). Neurophysiological activity arising from right and left IWAT nerve bundles was measured for 10 min prior to and then in response to a 15 μl injection of the β3 adrenergic receptor agonist CL316,243 (CL, 0.2 ng/kg or 0.1 ng/kg, 3.0 μl/min for 5 min) into one IWAT, while saline vehicle was simultaneously injected into the contralateral IWAT pad, CL stimulation is commonly used to simulate SNS activity to adipose tissue and reliably induces lipolysis *in vivo* and *in vitro* [21,22]. A separate cohort of animals was pretreated with the antilipolytic drug 3,5-dimethylpyrazole (DMP, 12 mg/kg, i.p.) [23–25] 20 min before IWAT infusions of CL (0.2 ng/kg) and saline. Eicosopentanoic acid (EPA) and arachidonic acid (AA) are both highly mobilized from adipose tissue during stimulated-lipolysis at ratios to other mobilized FAs that appear to be conserved across species [26,27]. Thus, EPA and AA were used as representative FAs—of potentially many more FA species—that may signal acute and local lipolysis to WAT afferents. Doses for EPA[2.94 μM in 15 μl Tocrisolve, ~8.91 mg/kg] and AA[0.27 μM in 15 μl Tocrisolve, ~0.81 mg/kg] were calculated from studies that measured net output of lipolytic products from adipose fragments in rats [27,28]; accordingly, physiologically relevant levels of EPA and AA were injected into WAT to assess whether lipolytic products stimulate WAT afferents directly. Infusions of drug or vehicle were counterbalanced by side to control for possible side bias of IWAT afferent innervations.

Extracellular signals were amplified 10,000 times with a differential AC amplifier set to low pass filter 100 Hz and high pass filter 1000 Hz (Model 1700; A-M Systems, Sequim, WA). Analog signals were visualized on an oscilloscope (Model 2530, BK Precision, Yorba Linda, CA), audio analyzer (Model 74-30-1; FHC, Bowdoin, ME), and digitized through a Digidata data acquisition system (Model 1440a; Molecular Devices, Sunnyvale, CA) at a 20,000 Hz sampling rate. Recordings were captured with accompanying Clampex 10.3 software and analyzed for the number of spikes based on a voltage threshold two standard deviations above mean non-signal noise via Clampfit 10.3 data analysis software package. All counted waveforms were visually screened, and non-physiological noise detected with the set threshold was identified and removed from analysis. Percentage change from baseline nerve activity was calculated for 10 min bins for each nerve recording session, then the difference between IWAT afferent activities from CL injected pads and saline injected pads was calculated and used for statistical analysis.

2.3. Western blot analysis of lipolysis induced by CL

Using an identical infusion protocol to bilateral electrophysiology experiments, but without IWAT afferent dissection/dissociation from the CNS, CL (0.1 ng/kg or 0.2 ng/kg) was infused into one IWAT pad simultaneously with a saline vehicle was infused into the contralateral IWAT pad. Animals receiving a high dose of CL (0.2 ng/kg) were pretreated with either DMP (20 min prior, 12 mg/kg, i.p.) or saline vehicle, and animals receiving a lower dose of CL (0.1 ng/kg)

 © 2016 The Author(s). Published by Elsevier GmbH. This is an open access article under the CC BY-NC-ND license (http://creativecommons.org/licenses/by-nc-nd/4.0/).

received no pretreatment. Fifteen minutes after the start of bilateral infusions (15 μl each pad, 3 loci, 3.0 μl/min for 5 min), ~100 mg of each IWAT pad was quickly removed, snap frozen in liquid nitrogen to preserve protein, then stored at −80 °C until analysis by Western blot.

Frozen adipose tissue samples were homogenized using microcentrifuge tubes containing 0.5 mm zirconium oxide beads homogenization buffer containing 50 mM HEPES, 100 mM NaCl, 10% SDS, 2 mM EDTA, 0.5 mM DTT, 1 mM benzamidine, protease inhibitor cocktail (Calbiochem, EMD Chemicals, Gibbstown, NJ), and phosphatase inhibitor cocktail (Thermo Fischer Scientific, Rockford, IL) at a ratio of 1:2 tissue weight (mg): homogenization buffer (μl). The samples were agitated 2 × 1 min using a bullet blender tissue homogenizer and then centrifuged at 13,000 g for 10 min at 4 °C. The infranatant was collected, aliquoted and stored at −80 °C until protein content was determined. Samples were diluted 1:10 in dH2O and the protein content of the tissue extract was determined using the bicinchoninic acid protein assay kit (Thermo Fisher Scientific, Rockford, IL). Samples containing 10 μg of protein were mixed with loading buffer and heated at 95 °C for 5 min, electrophoresed on a low-bis SDS-PAGE [10%: 0.08% acrylamide:bis] and transferred to polyvinylidene difluoride membranes. Membranes were cut in half so that immunoblotting could be done on duplicate lanes with different antibodies from the same gel. Cut membranes were incubated in Tris buffered-saline (TBS) with 4% nonfat dry milk and 0.3% Tween blocking solution for 2 h, then incubated in primary antibody at 4 °C (anti-ATGL, anti-HSL, anti-phospho-HSL, anti-beta-actin, 1:1000; Cell Signaling Technology, Danvers, MA) in TBS-4%milk-0.3% Tween for 2 days. Immunoblots were rinsed 4 × 5 min in TBS-Tween (TBST) and then incubated with secondary antibody (Anti-rabbit IgG HRP-linked antibody, 1:1000; Cell Signaling Technology, Danvers, MA) for 2 h at room temperature. The immunoblots were rinsed 3 × 10 min in TBST and then incubated with LumiGLO chemiluminescent kit (Cell Signaling Technology, Danvers, MA) to reveal bands.

2.4. Fast Blue (FB) labeling and CL administration

Siberian hamsters ($n = 10$) were anesthetized with ketamine/xylazine (100 mg/kg, 10 mg/kg; i.p.) and ventral lateral 2 cm incisions were made to expose both IWAT pads. The neuronal tracer FB (1.0%; EMS-CHEMIE GmbH, Gross-Umstadt, Germany) was injected with a microsyringe into eight separate loci (2 μl/locus) of the left and right IWAT. After the last injection, the incision was closed with sterile wound clips and ketofen (5 mg/kg, s.c.; Fort Dodge Animal Health, Fort Dodge, IA) was administered for 3 d postinjection to minimize postoperative discomfort.

One week later, CL (0.2 ng/kg in 0.9% sterile saline) was injected into one IWAT pad across eight separate loci with nearly simultaneous intra-contralateral IWAT injections of the saline vehicle (2 μl/locus for a total of 16 μl) served as a within animal control. Injections of drug or vehicle were counterbalanced by side to control for possible side bias of IWAT afferent innervations. The skin was gently pinched closed, and sterile saline-soaked gauze was laid over top of the incision site for 60 min until hamsters were sacrificed and DRGs processed for c-Fos immunohistochemistry.

2.5. Tissue fixation and c-Fos immunostaining on DRGs

Hamsters were euthanized by overdose with pentobarbital sodium (Sleep Away; 300 mg/kg) and transcardially perfused with 75 ml of 0.9% heparinized saline followed by 150 ml 4.0% paraformaldehyde in 0.1 M PBS, pH 7.4, directly into the aorta. The DRGs (T12-L2) were extracted, the epineurium debrided and postfixed in the same fixative for 15 min at 4 °C, then transferred to an 18.0% sucrose solution in 0.1 M PBS with 0.1% sodium azide and stored at 4 °C until they were sectioned at 20 μm on a freezing microtome. Sections were received directly onto slides (Superfrost Plus, VWR International) in three series with every fourth section on the same slide. This procedure yielded ~24 sections with each slide containing eight sections. Thus, an estimated total neuronal number per ganglion could be obtained by multiplying the number per section by 24 or averages by 8.

For DRG c-Fos immunostaining on slides, sections were rinsed in 0.1 M PBS (2 × 15 min) followed by 1 h blocking in 5.0% normal horse serum (NHS; Vector Laboratories) and 0.3% Triton X-100 in 0.1 M PBS. Sections were then incubated in primary rabbit anti-c-Fos (1:500; sc-52; Santa Cruz Biotechnology) antibody with 10.0% NHS and 0.3% Triton X-100 in 0.1 M PBS overnight. Next, the sections were incubated in secondary donkey anti-rabbit Cy3 (1:200; Jackson ImmunoResearch) for 3 h, rinsed with 0.1 M PBS (3 × 15 min) and coverslipped with ProLong Gold Antifade Reagent (Life Technologies). All steps were performed at room temperature.

2.6. Brown fat transponder implantation, temperature recordings, and acute surgical denervation of IWAT

Siberian hamsters ($n = 36$) were anesthetized with ketamine/xylazine (100 mg/kg, 10 mg/kg, i.p.) and a dorsal 2 cm interscapular incision was made to expose IBAT. One electronic transponder (Bio Medic Data Systems) with a built-in temperature sensor was gently implanted under one IBAT pad of each hamster, the temperature of which was read with a handheld DAS-7007R scanner (Bio Medic Data Systems) as we have used successfully previously [29–31]. The incision was closed with sterile wound clips.

After two weeks of recovery, hamsters were again anesthetized with ketamine/xylazine (100 mg/kg, 10 mg/kg, i.p.) then a ventral lateral 3 cm incision was made to expose right IWAT. Nerves innervating the ventral portion of IWAT were either left intact, or surgically destroyed [32] to test whether WAT lipolysis sensed by local afferents could drive BAT thermogenesis (diagram of procedure, Figure 6A). CL (0.2 ng/kg) or saline vehicle, was injected intra-right ventral IWAT exactly as above at three loci (5 μl/locus for a total of 15 μl). This dose was chosen based on neurophysiological recordings demonstrating dose-dependent IWAT afferent activation, Western blot data confirming increased lipolysis by significant pHSL/HSL increases of the pad delivered, and previous studies by us that determined CL microinjections of 0.2 ng/kg into IBAT did not affect core body temperature [29]. The incision was immediately covered with a warm saline-soaked gauze pad, animals were then moved to a circulating water warming pad set to 37 °C and remained there under heat lamp with ambient air surrounding the animals stable at ~35–36 °C. Temperature recordings from IBAT were started immediately after the animal reached the warming pad then monitored every 5 min for 1 h postinjection as done previously [29]. Core body temperature in these anesthetized animals was measured using a rectal temperature sensor connected to BAT-10 Thermometer (Physitemp Instruments).

3. DATA ANALYSIS

3.1. Neurophysiological recordings

The numbers of WAT afferent action potentials occurring as a function of time were integrated into either 30 s bins and compared across treatments for unilateral recordings, or 10 min bins for bilateral recordings, where the onset of infusion up to 20 min post infusion were compared against the pre-infusion 10 min baseline recordings. Percent change mean nerve activity from contralateral (vehicle-

 © 2016 The Author(s). Published by Elsevier GmbH. This is an open access article under the CC BY-NC-ND license (http://creativecommons.org/licenses/by-nc-nd/4.0/).

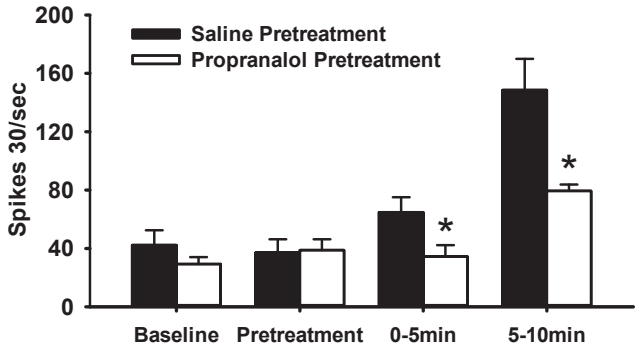

Figure 1: Glucoprivation increases IWAT multiunit nerve spiking in a β-AR dependent fashion. 2DG (500 mg/kg, i.p.) increased IWAT multiunit spiking, an effect blocked by pretreatment with β-AR antagonist propranolol. Bars represent number of spikes per 30 s of IWAT afferents in hamsters that received either propranolol (40 mg/kg, s.c.) or saline vehicle (s.c.) pretreatment prior to 2DG application. * different from saline pretreatment, $p < 0.05$.

infused) IWAT was compared using one-way ANOVA for each treatment from baseline nerve activity. Post hoc analysis of individual time points across experiments were compared using Student's *t* tests with Bonferroni correction via SigmaPlot (v12.3; Systat Software Inc., San Jose, CA). Results were considered significant if mean nerve activity in unilateral recordings—or percent change from baseline activity in bilateral recordings—differed from vehicle control, $p < 0.05$.

3.2. Western blot protein analysis

Band intensity was quantified based on optical densitometry measurements using ImageJ (US National Institutes of Health, Bethesda, MA). The values for HSL/actin, and pHSL/actin were collected and ratios of pHSL/HSL were compared using paired samples *t*-tests between ipsilateral and contralateral IWAT within animals via SigmaPlot (v12.3; Systat Software Inc., San Jose, CA). Data are displayed (Figure 3) as arithmetic change in pHSL/HSL for clarity of presentation. Results were considered significant if mean pHSL/HSL from CL-infused pads differed from their contralateral vehicle-infused control, $p < 0.05$.

3.3. c-Fos-ir and FB colocalization

All labeled cells from three central sections of each DRG were counted from captured images by experimenters blind to treatment conditions. Raw totals for each label (e.g., c-Fos and FB) as well as c-Fos+FB colocalized cells were compared between drug treatments using multiple Mann—Whitney U tests at each ganglionic level. In addition, the percentage of FB labeled cells expressing c-Fos were compared between drug treatments at each ganglionic level and combined across all ganglia to demonstrate the specificity of CL infusion to individual IWAT afferent neurons. Comparisons were considered statistically different when DRG labeling ipsilateral to CL infusion differed from the contralateral vehicle-infused counterpart, $p < 0.05$.

3.4. BAT and rectal temperature recordings

Temperature and change in temperature from the "0 min" time point were each analyzed by repeated measures two-way ANOVA by drug treatment and the state of IWAT neural connectivity. Preplanned comparisons between treatments at each time point were conducted

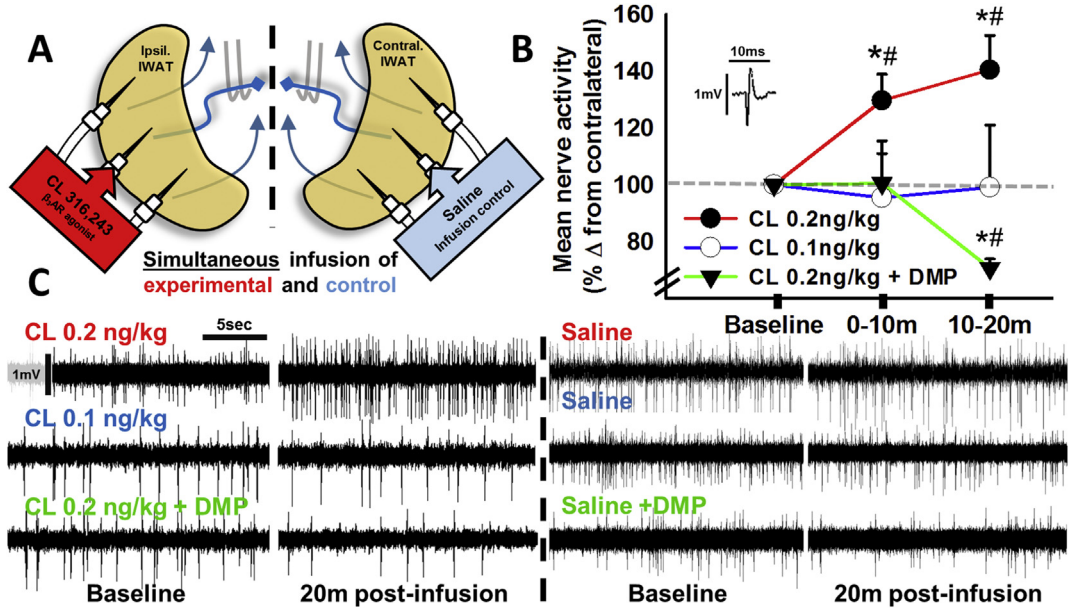

Figure 2: Intra-adipose β3-AR agonism increases IWAT multiunit nerve activity. (A) Diagrammatic representation of real-time *in vivo* bilateral multiunit electrophysiology of WAT afferent nerves. Afferent nerves resected from ventrally exposed IWAT (blue curved lines), cut proximal to electrodes (gray hook pairs) to eliminate efferent interference, and analyzed for multiunit spike frequency over time. Symmetrically placed infusion needles indicate bilateral simultaneous infusion of lipolytic drug CL316,243 (CL, β3-AR agonist) and its sterile saline vehicle (no drug) in the contralateral negative control pad. (B) CL dose-dependently increased IWAT multiunit spiking, an effect blocked by pretreatment with the antilipolytic drug 3,5-dimethylpyrazole (DMP, 12 mg/kg, i.p). Data are expressed as a percentage change of activity from CL-infused pad over contralateral to eliminate whole animal IWAT nerve variability caused by the recording/injection procedure. Inset is a representative single spike to display acquired waveforms. (C) Representative (20 s) traces from IWAT afferents and contralateral counterparts at baseline and 20 min post-infusion where the ipsilateral IWAT was infused with CL at either 0.2 ng/kg (top), 0.1 ng/kg (middle), or 0.2 ng/kg 20 min after pretreatment with antilipolytic drug DMP (bottom). CL injections were counterbalanced by side to control for any possible side bias. Scale bars on first trace apply to all traces. Dotted line separates ipsilateral vs contralateral IWAT afferent recordings from each of the three representative animals. * different from contralateral control; # different from baseline activity, $p < 0.05$.

 © 2016 The Author(s). Published by Elsevier GmbH. This is an open access article under the CC BY-NC-ND license (http://creativecommons.org/licenses/by-nc-nd/4.0/).

using multiple *student's t* test with Bonferroni correction. Comparisons were considered statistically different when temperature or change in temperature from baseline differed from animals whose IWAT was injected with saline and innervating nerves intact, $p < 0.05$.

4. RESULTS

2DG significantly increased neurophysiological activity of IWAT afferents in both 0–5 min and 5–10 min post-stimulus time intervals (*Student's t test with Bonferroni correction*; $n = 13$; baseline, $p = 0.143$; pretreatment, $p = 0.448$; 0–5 min, $p = 0.050$; 5–10 min, $p = 0.009$, Figure 1), and the 2DG-induced increase was blocked by pretreatment with propranolol relative to saline infusions.

IWAT administration of the high dose of CL (0.2 ng/kg, Figure 2B,C) also significantly increased neurophysiological spike activity beginning 5–10 min after the CL infusion, and lasting until the end of the recording session. IWAT neurophysiological spike activity was not increased in vehicle-injected contralateral IWAT or when CL was infused at a dose insufficient to induce lipolysis (0.1 ng/kg, Figures 2B,C and 3). DMP blocked the ability of a high dose of CL to stimulate WAT afferents, and interestingly inhibited their activity from

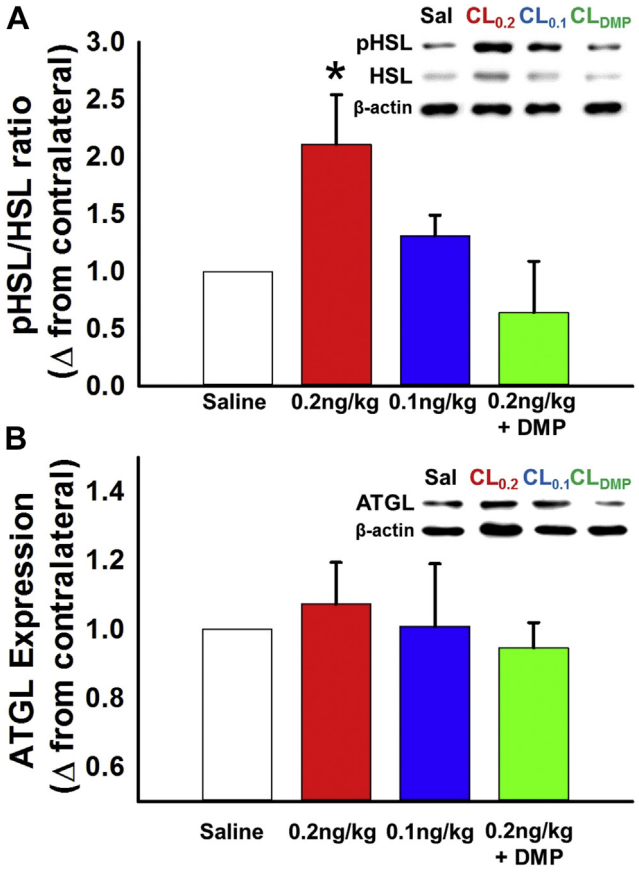

Figure 3: Intra-adipose CL increases pHSL/HSL indicating β_3-AR induced lipolysis. (A,B) Western blot analysis of the ratio of pHSL to HSL and ATGL reveals increased stimulated lipolysis with 0.2 ng/kg but not 0.1 ng/kg CL 15 min after infusion. In addition, pretreatment with DMP (i.p.) blocked CL stimulatory effects. Colored bars indicate (A) the mean ratio of pHSL to HSL and (B) ATGL in CL-injected IWAT compared with their saline-injected contralateral control IWAT (white bar). Error bars indicate SEM. Representative blots are provided as the inset with the label color and order of the bars used to indicate treatment (all units in ng/kg). * different from contralateral saline injected pad, $p < 0.05$.

10 to 20 min post-infusion (repeated measures ANOVA; CL 0.2 ng/kg, $n = 7$, $p = 0.002$; CL 0.1 ng/kg, $n = 4$, $p = 0.964$; CL 0.2 ng/kg + 12 mg/kg DMP, $n = 5$, $p = 0.158$; Student's t test with Bonferroni correction; CL 0.2 ng/kg, $n = 7$, 0–10 min, $p = 0.022$, 10–20 min, $p = 0.002$; CL 0.1 ng/kg, $n = 4$, 0–10 min, $p = 0.779$, 10–20 min, $p = 0.968$; CL 0.2 ng/kg + 12 mg/kg DMP, $n = 5$, 0–10 min, $p = 0.979$, 10–20 min, $p < 0.001$).

CL-induced lipolysis was confirmed by examining the change in ratios between pHSL and HSL using Western blot as a well-established marker for fat-pad-specific sympathetically dependent lipolysis [13,33]. CL infusion (0.2 ng/kg) increased pHSL: HSL after 15 min but did not affect pHSL: HSL when animals had been pretreated with DMP (12 mg/kg, CL 0.2 ng/kg) or CL only at a lower dose (0.1 ng/kg, Figure 3) (paired t tests; CL 0.2 ng/kg, $n = 17$, $p = 0.015$; CL 0.1 ng/kg, $n = 5$, $p = 0.193$; CL 0.2 ng/kg + 12 mg/kg DMP, $n = 5$, $p = 0.515$). ATGL did not differ among treatment groups ($p > 0.05$).

FB neurotracing and c-Fos colocalization revealed a specific activation of DRG neurons connected directly to IWAT on the side ipsilateral to the high dose of CL infusion (0.2 ng/kg, Figure 4A–F, J) despite nearly identical neurotracer labeling (Figure 4H) and only a trend toward higher overall c-Fos-ir (Figure 4I) (Mann–Whitney Rank Sum Tests; FB, T12, $n = 7$, $p = 0.905$; T13, $n = 7$, $p = 0.571$; L1, $n = 7$, $p = 0.556$; L2, $n = 7$, $p = 0.486$; L3, $n = 7$, $p = 0.286$; c-Fos-ir, T12, $n = 7$, $p = 0.556$; T13, $n = 7$, $p = 0.250$; L1, $n = 7$, $p = 0.111$; L2, $n = 7$, $p = 0.686$; L3, $n = 7$, $p = 0.905$; Colocalized, T12, $n = 7$, $p = 0.190$; T13, $n = 7$, $p = 0.502$; L1, $n = 7$, $p = 0.032$; L2, $n = 7$, $p = 0.030$; L3, $n = 7$, $p = 0.041$). In addition, the percent of FB labeled cells expressing c-Fos tended to increase in L3 but was significantly higher at ganglionic levels L1, L2, and overall across T12-L3 (Mann–Whitney Rank Sum Tests, T12, $n = 7$, $p = 0.215$; T13, $n = 7$, $p = 0.442$; L1, $n = 7$, $p = 0.032$; L2, $n = 7$, $p = 0.029$; L3, $n = 7$, $p = 0.063$; Total, $n = 35$, p = 0.001).

EPA, AA, and a cocktail of both together each significantly increased neurophysiological activity of IWAT afferent nerves (Figure 5) (repeated measures ANOVA; EPA, $n = 6$, $p = 0.013$; AA, $n = 3$, $p = 0.003$; EPA+AA cocktail, $n = 4$, $p = 0.005$). Post hoc analysis revealed lipolytic products EPA and AA each increased multiunit activity to a similar magnitude and latency of effect as the high dose of CL (Student's t test with Bonferroni correction; 0–10 min: EPA, $n = 6$, $p = 0.047$; AA, $n = 3$, $p = 0.019$; 10–20 min: EPA, $n = 6$, $p = 0.015$; AA, $n = 3$, $p = 0.003$).

IBAT temperature change from baseline was significantly increased after CL infusion in WAT pads with intact neural innervation (repeated measures ANOVA; $n = 36$, $p < 0.001$) as early as 5 min post infusion and persisted for every time point measured (Figure 6C). This effect was abolished when WAT was denervated before CL infusion and did not increase when saline was infused into denervated WAT (Figure 6C). Anesthetized hamsters experienced mild post anesthesia-induced hypothermia [34] after which IBAT (repeated measures ANOVA; $n = 36$, $p < 0.001$) and rectal raw temperatures (repeated measures ANOVA; $n = 36$, $p < 0.001$) slowly increased over time throughout the experiment (Figure 6B,D); however, neither IBAT (repeated measures ANOVAs; $n = 36$, $p < 0.183$) nor rectal (repeated measures ANOVA; $n = 36$, $p = 0.922$) raw temperatures differed among treatment groups at baseline or any subsequent time point measured (Figure 6B,D).

5. DISCUSSION

IWAT afferents are activated by 2DG-induced glucoprivation [9] and the present results show that this effect is attenuated by propranolol pretreatment, suggesting that β-AR-dependent lipolysis drives IWAT

 © 2016 The Author(s). Published by Elsevier GmbH. This is an open access article under the CC BY-NC-ND license (http://creativecommons.org/licenses/by-nc-nd/4.0/).

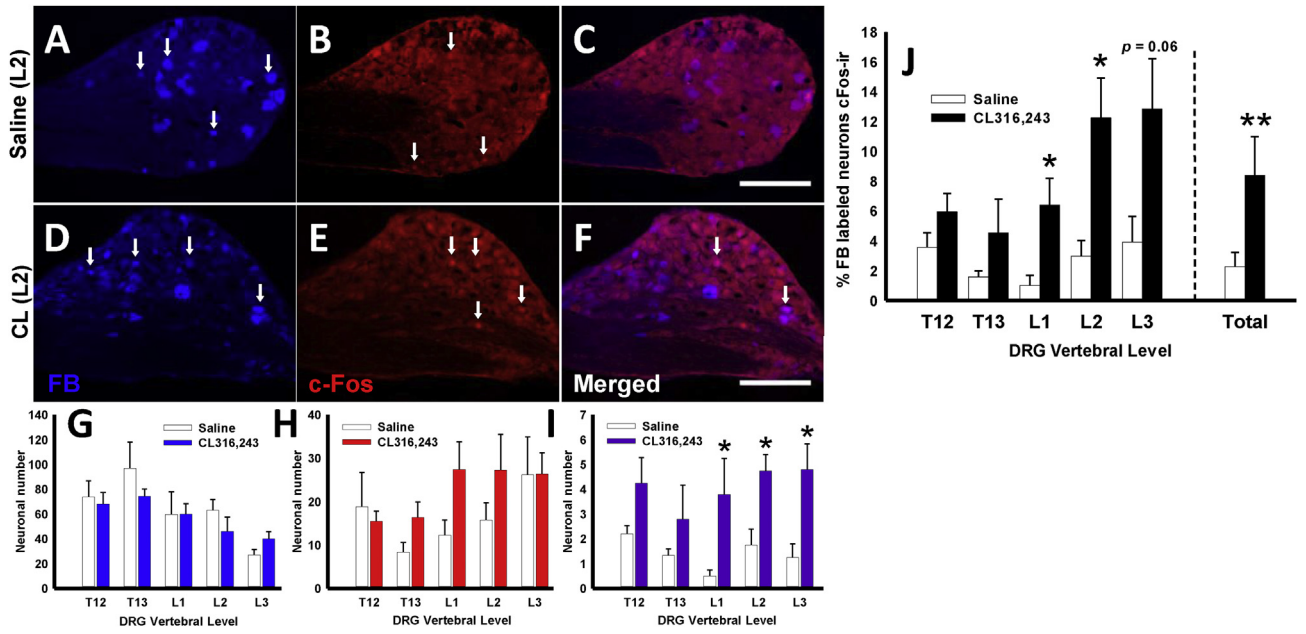

Figure 4: Intra-adipose β3-AR agonism increases c-Fos-ir in DRG neurons connected to IWAT. (A—F) Representative images of Fast Blue (FB, A, D) positive, c-Fos (B, E)-ir, and colocalized (C, F) neurons in DRG at the L2 vertebral level from the same animal both contralateral (top) and ipsilateral (bottom) to CL injections. Scale bar = 100 μm. White arrows indicate some but not all labeled cells of interest and rows are separated by treatment. (G—I) Neuronal number counted from three central-most sections of each DRG, each animal, and both treatments positive for FB (G), c-Fos-ir (H), or both (I). (J) Percentage of FB labeled neurons expressing c-Fos at each vertebral level (T12-L3) from animals injected with CL into their ipsilateral IWAT and saline vehicle into their contralateral IWAT. * different from contralateral DRGs innervating saline injected pads, $p < 0.05$; **$p < 0.001$.

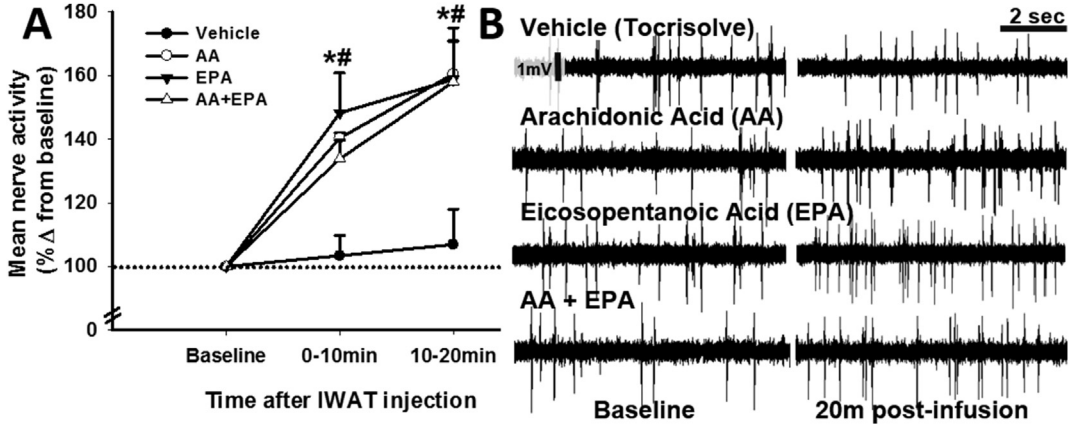

Figure 5: Intra-IWAT eicosopentanoic acid (EPA) and arachidonic acid (AA) increases IWAT multiunit nerve activity. (A) EPA, AA, and a mixture of EPA + AA all increased IWAT multiunit spiking with a similar magnitude and latency to effect. Data are expressed as a percentage change of activity from baseline nerve activity. (B) Representative (8 s) traces from IWAT afferents and contralateral counterparts at baseline and 20 min post-infusion. Scale bars on first trace apply to all traces. Dotted line separates ipsilateral vs contralateral IWAT afferent recordings from each of the three representative animals. * different from saline injected control; # different from baseline activity, $p < 0.05$.

afferent spiking (Figure 2B,C). IWAT afferent activation appears to depend on local CL-induced lipolysis, as evidenced by increases in: 1) WAT HSL phosphorylation, 2) neurophysiological spike activity of WAT afferents, and 3) c-Fos immunoreactivity in adipose tissue-connected sensory spinal neurons in the DRG. Furthermore, blocking CL-induced lipolysis with DMP pretreatment attenuated WAT CL-induced HSL phosphorylation (Figure 3A) and blocked IWAT afferent activation (Figure 2B,C). Although we did not observe increases in WAT ATGL protein content 15 min after CL injections, pHSL was significantly higher (Figure 3A,B) demonstrating enhanced β_3AR stimulation as an index of WAT lipolysis. To further support the hypothesis that lipolysis activates WAT afferents, we then tested two fatty acids known to be highly released during norepinephrine-induced lipid mobilization [27] and both EPA and AA were sufficient to drive WAT afferent neurophysiological activity in the absence of CL. These data together suggest that lipolysis products are sufficient to drive WAT afferent spiking, perhaps relaying the amount and types of released lipid to the CNS.

Using immunohistochemistry for CGRP and substance P as afferent nerve markers, sensory nerves identified within adipose tissue are predominantly located around major blood vessels and, less commonly, innervate the parenchymal adipose depot [35]. This observation is further illustrated by electron micrographs of the adipose cellular architecture where nerve fibers innervating the tissue primarily congregate around vasculature [2,36]. In the context of these anatomical findings, the present CL data support the suggestion that WAT afferent lipid sensors detect lipolytic products at the interface of

 © 2016 The Author(s). Published by Elsevier GmbH. This is an open access article under the CC BY-NC-ND license (http://creativecommons.org/licenses/by-nc-nd/4.0/).

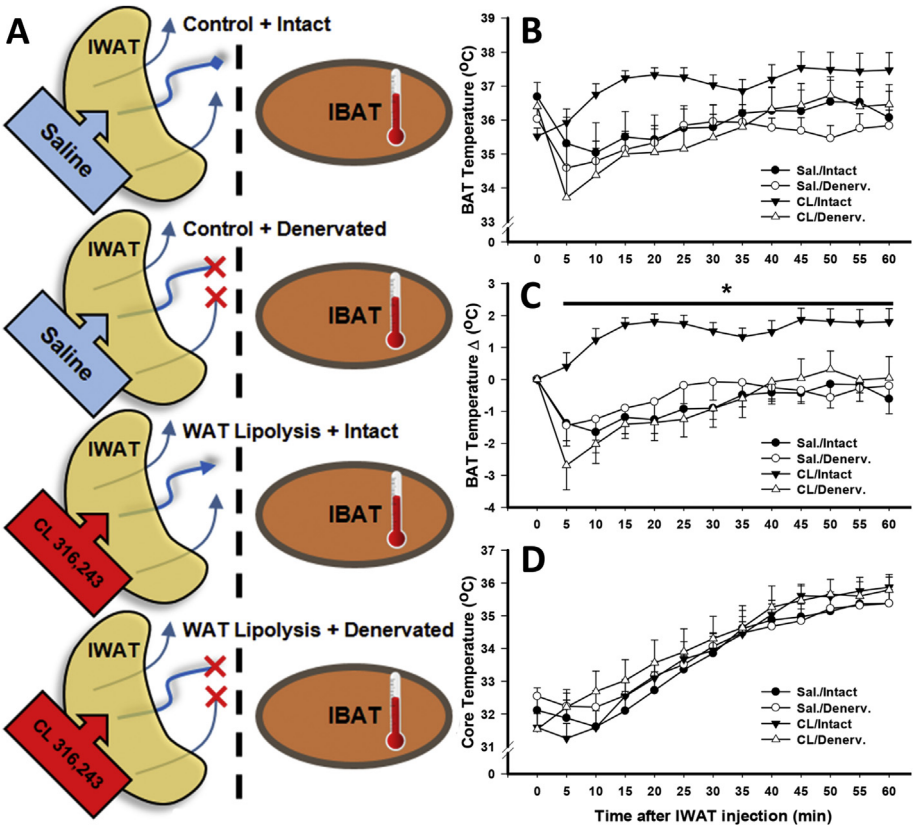

Figure 6: CL-induced IWAT afferent stimulation is sufficient to increase BAT thermogenesis. (A) Diagrammatic representation of the experimental setup. IWAT was either denervated or nerves left intact then injected with saline or a dose of CL316,243 (0.2 ng/kg) shown to increase IWAT afferent activity. (B) BAT temperature, (C) change in BAT temperature from baseline and (D) rectal temperature over the 60-min recording period. * different from saline-intact injected control, $p < 0.05$.

the adipose tissue with its blood supply. The possible role of WAT afferent lipid sensors around major blood vessels may be to inform the CNS about the quantity and types of lipid species entering circulation rather than their proximal release from individual adipocytes. Peripheral afferent nerves may also release CGRP into their innervating tissues, and may thereby act on adipose tissue WAT afferents. However, it is unknown whether decentralizing afferent fibers in this study modulates CGRP release or action either on adipocytes or WAT sensory nerves. Interestingly, CGRP injected directly into BAT attenuates norepinephrine-induced thermogenesis and is innately released by BAT afferent activation to this effect [37]. This suggests that afferents possibly regulate adipose function via negative feedback [37]. Despite these effects in BAT, we believe that our within-animal design employed during neurophysiological recordings mitigates the confounding effects of WAT afferent neuropeptide release in this study.

To identify putative physiological roles for this newfound sensory signal, we tested for the existence of a functional neuroanatomical linkage between WAT and BAT. Surgical denervation of WAT blocked BAT temperature increases during WAT CL-infusions (Figure 6A—D), demonstrating for the first time that WAT sensory signals contribute to BAT thermogenesis (Figure 6A—D). The present results are consistent with and expand upon prior data suggesting functional neuroanatomical sensory motor circuits linked to BAT thermogenesis. Indeed, whole-animal capsaicin-desensitization diminishes BAT thermogenic capacity [38] and causes atrophy of BAT [39]. Further, direct BAT sensory denervation produces similar BAT deficiency [40]. WAT to BAT neural circuitry may induce BAT thermogenesis either by directly increasing efferent SNS neural activity to BAT [39,41], or via increased adrenal release of norepinephrine [42]. Regardless of the precise neuroanatomical or neurohumoral pathways by which WAT CL infusion triggers BAT thermogenesis, we identify an acute and robust thermogenic response by BAT as a possible novel SNS output of the adipose afferent reflex (AAR) [43].

Earlier reports by us and others [4,11] suggest that WAT afferents activated by leptin presumably relay an inventory signal to the brain but also increase blood pressure via the AAR [43], whereas we now provide evidence that WAT afferents are activated by the local release of lipid and are sufficient to increase BAT temperature. Taken together, these reports identify heterogeneity among WAT afferents. It is still unclear whether single WAT afferent neurons are receptive to both leptin and lipids, and whether there are distinct neurons that sense and generate these different reflex outcomes. The existence of apparently distinct AAR outputs suggest that lipolysis-activated WAT afferents also increase blood pressure and thereby facilitate newly released lipid distribution throughout the body, to fuel BAT thermogenesis. Such a system may allow us to better understand mechanisms of SNS dysregulation in human obesity (*i.e.,* wherein SNS is overactive and stimulated-lipolysis is high [13]).

6. CONCLUSIONS

Taken together, these results provide evidence that WAT afferents—shown by us and others to be involved in 1) SNS feedback regulation to multiple tissues [4,7], 2) SNS-induced hypertension [43], 3) neural SNS feedback loops that are sensitive to insulin [44], 4) regulation of fat deposition throughout the body [45], 5) and food

 © 2016 The Author(s). Published by Elsevier GmbH. This is an open access article under the CC BY-NC-ND license (http://creativecommons.org/licenses/by-nc-nd/4.0/).

intake regulation [46]—increase their activity in response to the basic biological process of stimulated lipolysis (*i.e.,* simulated SNS outflow). In addition, one function of these lipolysis-activated WAT afferents is to increase BAT temperature in an acute fashion: a circuit which perhaps exists to correctly time the release of FFAs from WAT with the engagement of thermogenic machinery in BAT. This novel sensory signal has implications for many past and present studies examining the neural control of energy balance during physiological challenges where SNS-induced lipolysis is high (*e.g.,* food deprivation, cold exposure, and glucoprivation) [47]; therefore, we must continue to consider this synchrony of organ systems to more wholly understand homeostatic mechanisms of survival during energy challenges.

AUTHOR CONTRIBUTIONS

T.J.B., J.T.G., and G.J.S. designed and performed the neurophysiological recording experiments, L.A.S., J.T.G. performed the western blot lipolysis assays. J.T.G., V.R. performed the neurotracing experiments. J.T.G. performed the lipolysis induced brown adipose tissue temperature experiments. J.T.G., V.R., L.A.S., B.X. and G.J.S. wrote the paper. Supported by NIH R37DK035254 to T.J.B., NIH DK105441-01 to G.J.S., and NIH R01DK035254 to B.X.

ACKNOWLEDGMENTS

We thank Dr. Chun Jiang (Georgia State University) for his technical assistance and advise, Rachel Stanford for her help with data collection and analysis, and GSU Department of Animal Resources for maintaining the health and wellness of our laboratory animals.

CONFLICT OF INTEREST

The authors declare no competing financial interests.

REFERENCES

[1] Youngstrom, T.G., Bartness, T.J., 1995. Catecholaminergic innervation of white adipose tissue in the Siberian hamster. American Journal of Physiology 268:R744—R751.

[2] Giordano, A., et al., 1996. Tyrosine hydroxylase, neuropeptide Y, substance P, calcitonin gene-related peptide and vasoactive intestinal peptide in nerves of rat periovarian adipose tissue: an immunohistochemical and ultrastructural investigation. Journal of Neurocytology 25:125—136.

[3] Fishman, R.B., Dark, J., 1987. Sensory innervation of white adipose tissue. American Journal of Physiology 253:R942—R944.

[4] Niijima, A., 1998. Afferent signals from leptin sensors in the white adipose tissue of the epididymis, and their reflex effect in the rat. Journal of the Autonomic Nervous System 73(1):19—25.

[5] Caro, J.F., et al., 1996. Leptin: the tale of an obesity gene. Diabetes 45(11): 1455—1462.

[6] Shi, Z., et al., 2012. Sympathetic activation by chemical stimulation of white adipose tissues in rats. Journal of Applied Physiology 112(6):1008—1014.

[7] Niijima, A., 1999. Reflex effects from leptin sensors in the white adipose tissue of the epididymis to the efferent activity of the sympathetic and vagus nerve in the rat. Neuroscience Letters 262(2):125—128.

[8] Bartness, T.J., Song, C.K., 2007. Brain-adipose tissue neural crosstalk. Physiology and Behavior 91:343—351.

[9] Song, C.K., Schwartz, G.J., Bartness, T.J., 2009. Anterograde transneuronal viral tract tracing reveals central sensory circuits from white adipose tissue. American Journal of Physiology. Regulatory, Integrative and Comparative Physiology 296(3):R501—R511.

[10] Vaughan, C.H., Shrestha, Y.B., Bartness, T.J., 2011. Characterization of a novel melanocortin receptor-containing node in the SNS outflow circuitry to brown adipose tissue involved in thermogenesis. Brain Research 1411:17—27.

[11] Murphy, K.T., et al., 2013. Leptin-sensitive sensory nerves innervate white fat. American Journal of Physiology — Endocrinology and Metabolism 304(12): E1338—E1347.

[12] Ryu, V., Bartness, T.J., 2014. Short and long sympathetic-sensory feedback loops in white fat. American Journal of Physiology. Regulatory, Integrative and Comparative Physiology.

[13] Bartness, T., et al., 2014. Neural innervation of white adipose tissue and the control of lipolysis. Frontiers in Neuroendocrinology 35(4):473—493.

[14] Migliorini, R.H., et al., 1992. Control of adipose tissue lipolysis in ectotherm vertebrates. American Journal of Physiology 263(4 Pt 2):R857—R862.

[15] Lafontan, M., et al., 1997. Adrenergic regulation of adipocyte metabolism. Human Reproduction 12(Suppl 1):6—20.

[16] Bartness, T., Song, C.K., 2007. Thematic review series: adipocyte biology. Sympathetic and sensory innervation of white adipose tissue. Journal of Lipid Research 48(8):1655—1672.

[17] Belfrage, P., et al., 1981. Regulation of adipose-tissue lipolysis by phosphorylation of hormone-sensitive lipase. International Journal of Obesity 5(6): 635—641.

[18] Lass, A., et al., 2011. Lipolysis - a highly regulated multi-enzyme complex mediates the catabolism of cellular fat stores. Progress in Lipid Research 50(1):14—27.

[19] Haemmerle, G., et al., 2006. Defective lipolysis and altered energy metabolism in mice lacking adipose triglyceride lipase. Science 312(5774):734—737.

[20] Labbé, S., et al., 2015. In vivo measurement of energy substrate contribution to cold-induced brown adipose tissue thermogenesis. The FASEB Journal 29(5):2046—2058.

[21] Atgie, C., et al., 1998. Effects of chronic treatment with noradrenaline or a specific beta3-adrenergic agonist, CL 316 243, on energy expenditure and epididymal adipocyte lipolytic activity in rat. Comparative Biochemistry and Physiology Part A: Molecular & Integrative Physiology 119(2):629—636.

[22] Umekawa, T., et al., 1997. Effect of CL316,243, a highly specific beta (3)-adrenoceptor agonist, on lipolysis of epididymal, mesenteric and subcutaneous adipocytes in rats. Endocrine Journal 44:181—185.

[23] Masiello, P., et al., 2002. The antilipolytic agent 3,5-dimethylpyrazole inhibits insulin release in response to both nutrient secretagogues and cyclic adenosine monophosphate agonists in isolated rat islets. Metabolism 51(1):110—114.

[24] Locci-Cubeddu, T., Bergamini, E., 1983. Effects of antilipolytic agents on peroxisomal beta-oxidation of fatty acids in rat liver. Biochemical Pharmacology 32(11):1807—1809.

[25] Gerritsen, G.C., Dulin, W.E., 1965. Effect of a new hypoglycemic agent, 3,5-dimethylpyrazole, on carbohydrate and free fatty acid metabolism. Diabetes 14:507—515.

[26] Conner, W.E., Lin, D.S., Colvis, C., 1996. Differential mobilization of fatty acids from adipose tissue. Journal of Lipid Research 37(2):290—298.

[27] Raclot, T., Groscolas, R., 1993. Differential mobilization of white adipose tissue fatty acids according to chain length, unsaturation, and positional isomerism. Journal of Lipid Research 34(9):1515—1526.

[28] Raclot, T., et al., 1995. Selectivity of fatty acid mobilization: a general metabolic feature of adipose tissue. American Journal of Physiology 269: R1060—R1067.

[29] Ryu, V., et al., 2015. Brown adipose tissue has sympathetic-sensory feedback circuits. The Journal of Neuroscience 35(5):2181—2190.

[30] Brito, M.N., et al., 2007. Differential activation of the sympathetic innervation of adipose tissues by melanocortin receptor stimulation. Endocrinology 148(11):5339—5347.

 © 2016 The Author(s). Published by Elsevier GmbH. This is an open access article under the CC BY-NC-ND license (http://creativecommons.org/licenses/by-nc-nd/4.0/).

[31] Song, C.K., et al., 2008. Melanocortin-4 receptor mRNA expressed in sympathetic outflow neurons to brown adipose tissue: neuroanatomical and functional evidence. American Journal of Physiology 295:R417—R428.
[32] Vaughan, C.H., et al., 2014. Analysis and measurement of the sympathetic and sensory innervation of white and brown adipose tissue. Methods in Enzymology 537:199—225.
[33] Buettner, C., et al., 2008. Leptin controls adipose tissue lipogenesis via central, STAT3-independent mechanisms. Nature Medicine 14(6):667—675.
[34] Shimizu, Y., Saito, M., 1991. Activation of brown adipose tissue thermogenesis in recovery from anesthetic hypothermia in rats. American Journal of Physiology 261(2 Pt 2):R301—R304.
[35] De, M.R., Ricquier, D., Cinti, S., 1998. TH-, NPY-, SP-, and CGRP-immunoreactive nerves in interscapular brown adipose tissue of adult rats acclimated at different temperatures: an immunohistochemical study. Journal of Neurocytology 27(12):877—886.
[36] Cinti, S., 1999. The adipose organ. Milano: Editrice Kurtis.
[37] Osaka, T., et al., 1998. Temperature- and capsaicin-sensitive nerve fibers in brown adipose tissue attenuate thermogenesis in the rat. Pflugers Archiv 437(1):36—42.
[38] Giordano, A., et al., 1998. Sensory nerves affect the recruitment and differentiation of rat periovarian brown adipocytes during cold acclimation. Journal of Cell Science 111:2587—2594.
[39] Cui, J., Himms-Hagen, J., 1992. Rapid but transient atrophy of brown adipose tissue in capsaicin-desensitized rats. American Journal of Physiology 262: R562—R567.
[40] Vaughan, C., Bartness, T., 2012. Anterograde transneuronal viral tract tracing reveals central sensory circuits from brown fat and sensory denervation alters its thermogenic responses. American Journal of Physiology Regulatory, Integrative and Comparative Physiology 302(9):R1049—R1058.
[41] Cui, J., Zaror-Behrens, G., Himms-Hagen, J., 1990. Capsaicin desensitization induces atrophy of brown adipose tissue in rats. American Journal of Physiology 259:R324—R332.
[42] Bartness, T.J., Ryu, V., 2015. Neural control of white, beige and brown adipocytes. International Journal of Obesity Supplements 5(Suppl 1):S35—S39.
[43] Xiong, X.Q., Chen, W.W., Zhu, G.Q., 2014. Adipose afferent reflex: sympathetic activation and obesity hypertension. Acta Physiologica (Oxford) 210(3): 468—478.
[44] Ding, L., et al., 2015. Adipose afferent reflex response to insulin is mediated by melanocortin 4 type receptors in the paraventricular nucleus in insulin resistance rats. Acta Physiologica (Oxford).
[45] Shi, H., Bartness, T.J., 2005. White adipose tissue sensory nerve denervation mimics lipectomy-induced compensatory increases in adiposity. American Journal of Physiology 289:R514—R520.
[46] Yamada, T., et al., 2006. Signals from intra-abdominal fat modulate insulin and leptin sensitivity through different mechanisms: neuronal involvement in food-intake regulation. Cell Metabolism 3(3):223—229.
[47] Dunn, T.N., Adams, S.H., 2014. Relations between metabolic homeostasis, diet, and peripheral afferent neuron biology. Advances in Nutrition: An International Review Journal 5(4):386—393.

 © 2016 The Author(s). Published by Elsevier GmbH. This is an open access article under the CC BY-NC-ND license (http://creativecommons.org/licenses/by-nc-nd/4.0/).